Cement and Concrete Research 41 (2011) 263–269

Contents lists available at ScienceDirect

Cement and Concrete Research

journal homepage: http://ees.elsevier.com/CEMCON/default.asp

Physical and microstructural aspects of iron sulfide degradation in concrete

Thomas Schmidt [a,c,*], Andreas Leemann [b], Emanuel Gallucci [a], Karen Scrivener [a]

[a] EPFL, Swiss Federal Institute of Technology, Laboratory of Construction Materials, 1015 Lausanne, Switzerland
[b] Empa, Swiss Federal Laboratories for Material Testing and Research, 8600 Dübendorf, Switzerland
[c] Holcim (Schweiz) AG, Product development / -management, 5303 Würenlingen, Switzerland

ARTICLE INFO

Article history:
Received 16 April 2010
Accepted 17 November 2010

Keywords:
Concrete
Durability
Iron sulfide
Pyrite
Aggregates

ABSTRACT

The microstructural aspects of iron sulfide degradation in dam concrete were investigated by scanning electron microscopy (SEM) and energy dispersive spectroscopy (EDS) in both dam concrete samples and laboratory concrete. The results show that iron sulfide inclusions with a diameter of a few micrometers in the aggregates are reactive and appear to generate expansion first in the aggregates and consequently in the cement paste. The expansion from the iron sulfides is a consequence of the increase in volume of the reaction products formed. The types of iron sulfide present in the aggregate, mainly pyrrhotite (FeS) and pyrite (FeS_2), show similar reaction behavior in the aggregates. The released sulfate can lead to a secondary ettringite formation in the concrete matrix, but the degradation associated with this appears to be minor. The reaction of the iron sulfides was found to be very slow even when laboratory samples were exposed to elevated temperatures.

1. Introduction

Iron sulfides are common minor constituents in many rock types. They have been implicated in causing damage in concrete due to expansion [1]. It is usually assumed that oxidation of the iron sulfide leads to the release of sulfate ions causing internal sulfate attack in the concrete with expansive ettringite formation [2–5]. However, the microstructural aspects of this process have not been examined in detail.

The oxidation of iron sulfides like ironmonosulfide (FeS), pyrrhotite, and irondisulfide (FeS_2), pyrite, in concrete structures is a complex process that involves a sequence of different chemical reactions [6]. In the presence of oxygen and moisture, iron sulfides are unstable and oxidize to form iron oxides as shown by reactions 1 and 2:

$$2FeS + 2H_2O + 4.5O_2 \rightarrow Fe_2O_3 + 2H_2SO_4 \quad (1)$$

$$2FeS_2 + 4H_2O + 7.5O_2 \rightarrow Fe_2O_3 + 4H_2SO_4 \quad (2)$$

These reactions release sulfuric acid, which may go on to react with the cement paste and the iron oxides formed may also form hydroxides in the moist environment of the concrete.

Some research has been done on the factors affecting solubility as well as the nature of the intermediate and final reaction products of iron sulfides [7–10]. It was found that increasing concentration of molecular oxygen, higher alkalinity (pH), and smaller particle sizes accelerate the degradation of iron sulfides. The reaction kinetics of iron sulfides were found to depend on different parameters of the concrete such as porosity, inhomogeneity, and moisture conditions [7,11]. The solubility of the iron sulfide minerals was found to be about four times higher for FeS than FeS_2 [12,13].

The present study focuses on the microstructural aspects of concrete degradation due to iron sulfides inclusions in aggregates. This was studied in concrete cored from a dam and in concrete prepared from similar aggregates and stored in water bath at 60 °C for 5 years. The study indicates that the oxidation process of the iron sulfide causes cracking directly within the aggregates. The formation of secondary ettringite in the cement paste component was observed, but this did not seem to be a major cause of degradation.

2. Materials and methods

2.1. Field and laboratory samples

The study was carried out on two different concretes, concrete from a dam and concrete prepared from similar aggregates in the laboratory. The dam has a length of 290 m and an overall height of 36 m. Since the construction of the dam in the beginning of the 1970s, it has been monitored continuously for more than 40 years. It was observed that since the early 1980s, the concrete is steadily expanding. The upstream displacement of the dam in 1998 is 20 mm at the top and about 5 mm in the middle gallery (Fig. 1). Today the respective values are 45 and 10 mm. The overall expansion in the upper part of the dam is estimated to be 0.025%. However, it should be noted that the measured expansion only accounts for two

* Corresponding author. EPFL, Swiss Federal Institute of Technology, Laboratory of Construction Materials, 1015 Lausanne, Switzerland. Tel.: +41 58 850 57 80; fax: +41 58 850 55 71.
E-mail address: thomas.schmidt@holcim.com (T. Schmidt).

0008-8846/$ – see front matter © 2010 Elsevier Ltd. All rights reserved.
doi:10.1016/j.cemconres.2010.11.011

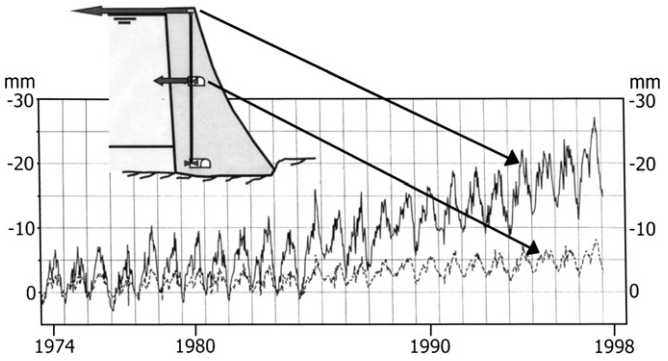

Fig. 1. Continuous expansion and movement upstream the dam since 1974.

dimensions, in horizontal arch dimension and in vertical dimension, and no estimation about the overall volume change of the dam can be made due to the lack of the data in the third dimension. Copious deposit of "rust" (iron oxides and hydroxides) accumulated in the galleries of the dam, and there was also a smell of sulfurous compounds.

Previous investigations of the concrete and the aggregates showed only some slight signs of ASR reactivity [14]. The concrete was produced with an ordinary Portland cement (equivalent to present day CEM I 32.5) using a water-to-cement ratio in the range 0.5–0.6. The samples (cores of 150 mm diameter) were taken from the downstream face and from galleries in the inner part of the 40 years old structure.

In addition, laboratory samples were produced from quarried (virgin) aggregates similar to those used for the construction of the dam. The cement used for the laboratory samples was ordinary Portland cement (CEM I 42.5) with a water to cement ratio of 0.50. A typical cement content in dam concrete in Switzerland is in the range of 280 kg/m^3 with a water-to-cement ratio of 0.5–0.6. As such, an aggregate content of about 1900 kg/m^3 can be estimated. The samples for the microstructural investigation were taken from concrete prisms ($70\times70\times280$ mm^3) stored in water for 5 years at 60 °C. Unfortunately the degree of expansion could not be assessed accurately in the laboratory samples.

For the microstructural investigation, selected samples were cut into sections and stored in isopropanol for 24 h at 20 °C. The SEM samples preparation included pre-polishing, impregnation with epoxy resin, polishing (9, 3, 1 μm), and carbon coating.

For the petrographic analysis, a number of 210 particles (grain size 8–32 mm) of virgin and extracted aggregates were prepared. Additionally, aggregates (grain size 8–16 mm) were embedded in epoxy resin, and thin sections were produced for optical microscopy and scanning.

2.2. Analytical methods

The petrography of the aggregates was determined according to Swiss standard SN 670'115. The thin sections of the embedded aggregates were analyzed using a Zeiss Axioplan light microscope, and they were additionally scanned with a flatbed scanner at a resolution of 2400 dpi. The scanned images were segmented based on their grey scale value in order to determine the amount of ores present.

The microstructure of the concrete samples was examined by scanning electron microscopy SEM (FEI QUANATA 200) using back-scattered electron imaging (BSE) and energy dispersive X-ray spectroscopy (EDS). The chemical analysis using EDS was done with a Li/Si crystal detector and an accelerating voltage of 15 kV.

The iron sulfide degradation was studied by EDS point analysis (corrected with phase standards) to determine the elements iron sulfur and oxygen. Carbon was excluded to eliminate the effects of the resin and microporosity. The atomic ratios S/Fe and O/Fe were plotted to indicate the iron phases present in the microstructure.

Table 1
Petrography of the quarried aggregate and the aggregate extracted from the concrete dam.

Type	Aggregate [% by number]	
	Virgin	From cores
Biotite schist 1	22	14
Biotite schist 2	41	60
Biotite schist 3	21	8
Muscovite schist	16	14
Granite	–	2
Dolomite	–	2

The image analysis IA was carried out on grey level images in combination with the chemical analysis using EDS mappings for the elements iron and sulphur. The iron sulfide inclusions were distinguished based on their brightness in the grey level histogram in combination with the chemical analysis.

3. Results and discussion

3.1. Petrography of the aggregates

The extracted and quarried aggregates consisted mainly of schists (Table 1). The foliation layers had a thickness of 0.5–2.0 mm. The schists were mainly composed of feldspar, quartz, biotite, and muscovite. Based on their relative amount of phyllosilicates and their texture, four different types could be distinguished. Biotit schist 1 contained mainly biotite and only little muscovite as phyllosilicates. Biotite schist 2 and 3 had the same mineralogy, but biotite schist 3 contains feldspar agglomerates of a diameter up to 5 mm. The relative amount of the different types of schist present showed that the extracted and the quarried aggregates are not identical but very similar.

Only a small part of the feldspars showed metamorphous degradation. The amount of microcrystalline quartz present in the aggregates was small. However, the quartz showed undulary extinction and sometimes poorly defined grain boundaries with irregular shapes (Fig. 2). The phyllosilicates were concentrated in cleavage planes. Some of the biotite was altered to chlorite. The amount of ores in the extracted and the quarried aggregates was analyzed to be about 0.3 to 0.4% by volume respectively. The size of the ore inclusions was in the range of 30 to 200 μm. Pyrite/marcasite and pyrrhotite were the most frequent ones with some minor amounts of illmenite ($FeTiO_3$) present. Pyrite/marcasite and pyrrhotite are referred to as iron *di*sulfide and iron *mono*sulfide, respectively, in the following text.

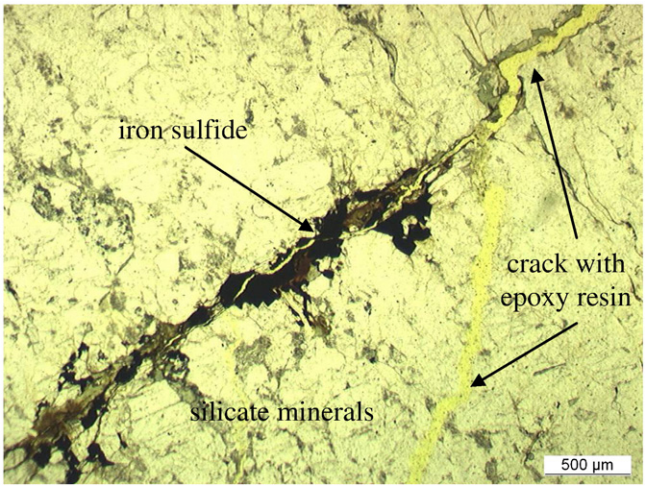

Fig. 2. Thin section of a typical aggregate in the dam concrete with iron sulfide inclusion (ore, dark areas).

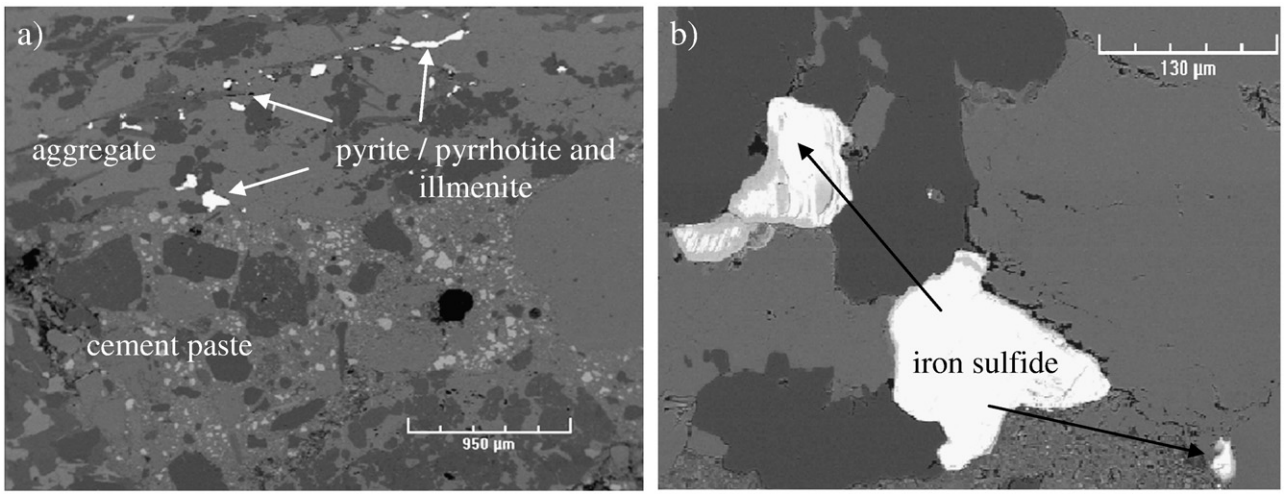

Fig. 3. Backscattered electron images (BSE) of concrete matrix from (a) dam concrete with iron sulfides and titanium oxide inclusions and (b) aggregate with iron sulfide particles present in laboratory concrete stored at 60 °C.

3.2. Sulfide inclusions and reaction

The microstructural investigations confirmed that some aggregates in the concrete contained iron sulfides as iron *mono*- and iron *di*sulfide (both reactive) and minor titanium oxide (nonreactive) inclusions. Both the titanium oxides and the iron sulfides were found to be randomly dispersed and agglomerated within the aggregates (Fig. 3a).

The investigation indicated that the deterioration process of the iron sulfide particles in various concrete samples was similar but not uniform. The oxidation or degradation process of both iron *mono*- and iron *di*sulfide usually started from the surface of the particles leading

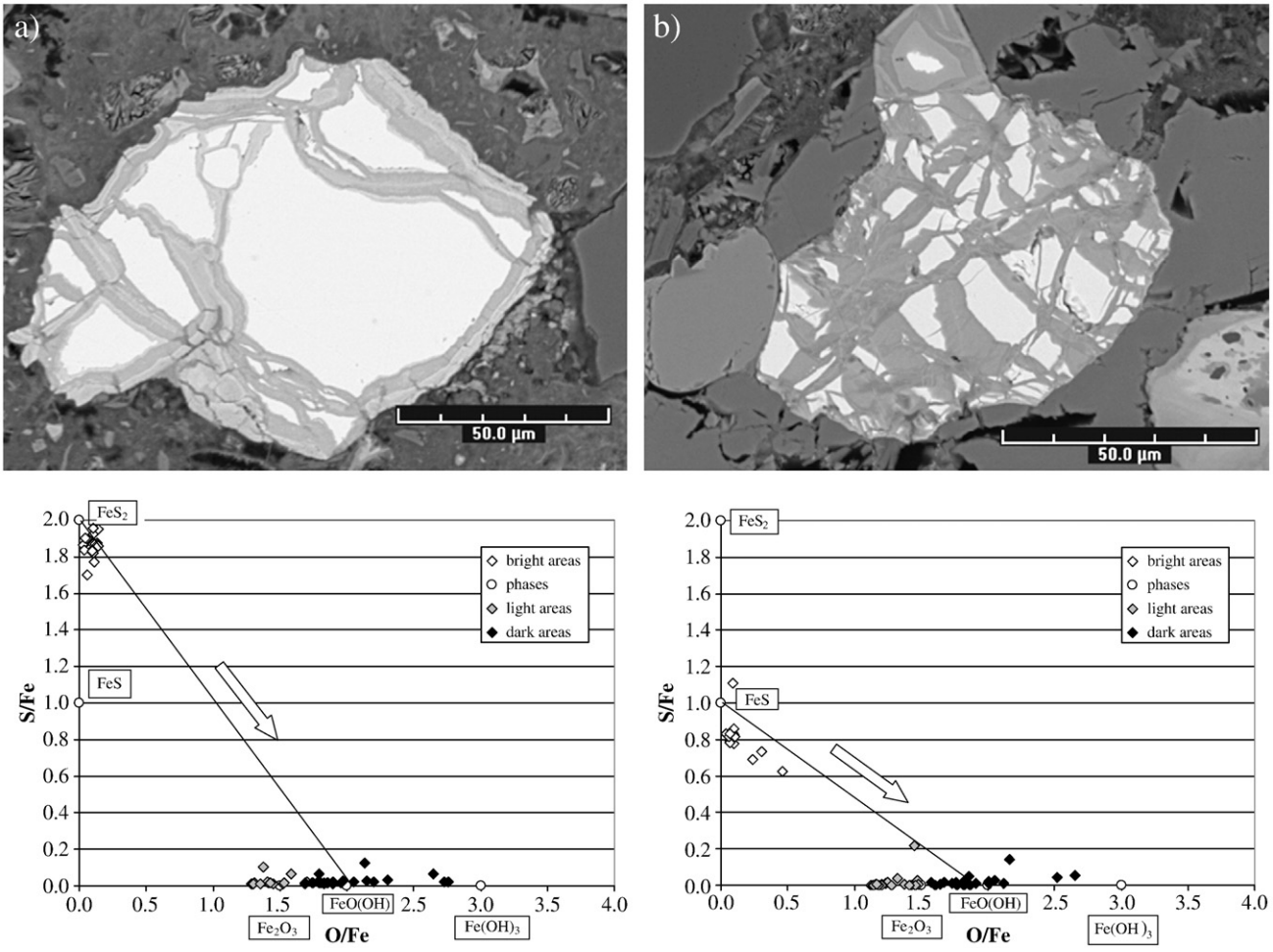

Fig. 4. Backscattered electron images (BSE) of an iron sulfides and EDS analysis of a) pyrite (FeS_2) and b) pyrrhotite (FeS) during the degradation process.

a) $2FeS + 2H_2O + 4.5O_2 \rightarrow Fe_2O_3 + 2H_2SO_4$

b) $2FeS_2 + 4H_2O + 7.5O_2 \rightarrow Fe_2O_3 + 4H_2SO_4$

$Fe_2O_3 + H_2O \rightarrow 2FeO(OH)$

$2FeO(OH) + 2H_2O \rightarrow 2Fe(OH)_3$

Fig. 5. Summary of the observed reaction sequence of pyrrhotite (FeS) and pyrite (FeS_2) during the oxidation/degradation process involving oxygen and moisture.

to a layer of oxidation products, which are darker than the unreacted iron sulfide (see micrographs (a) and (b) in Fig. 4). The different grey levels already give an insight of the change in the chemical composition and the replacement of the sulfide. From the chemical microanalyses, the iron sulfide particles seem to react first to form iron oxide (Fe_2O_3) and secondly iron hydroxides ($FeO(OH)$, $Fe(OH)_3$) as summarized in Fig. 5. Thus the different grey levels indicate the replacement of the sulfide ions by oxygen and hydrogen ions. The oxidation or degradation reaction was found to usually start from the outside inwards of the iron sulfides particles (Fig. 6).

From the quantitative analysis, the total amount of iron sulfides present in the dam aggregates (extracted and quarried) was analyzed to be 0.28% by volume, which is in a very good agreement to the results from the petrographic analysis. More detailed investigations revealed that about 80% by volume of the iron sulfides were present as iron monosulfide (pyrrhotite, FeS) and about 20% by volume as iron disulfide (pyrite, FeS_2). The image analysis further revealed that only about 30% to 40% by volume of the total iron sulfides of the extracted aggregates had reacted after more than 40 years in the dam concrete. However, the reaction kinetics can be assessed only qualitatively (see Section 3.3.1).

The laboratory concrete samples (4 years old) had the same appearance and pattern of reaction as the dam concrete (40 years old), but the extent of reaction of the iron sulfides was much lower in the laboratory samples (Fig. 3b). The reaction products as analyzed with EDS show the same composition of the reaction products in laboratory and dam concrete. These observations clearly indicate a very slow reaction rate of the iron sulfide inclusions and the difficulties to reproduce the iron sulfide degradation in the laboratory scale. Due to the low degree of reaction, it was not possible to assess the influence of temperature on kinetics. Therefore, a direct comparison between the concrete in the dam and the laboratory samples is not possible.

3.3. Manifestation of damage in the microstructure

3.3.1. Aggregate reaction

The concrete samples further showed significant cracking of the aggregates. It appeared that most of the cracks originated from iron sulfide containing regions within the aggregates and then extended

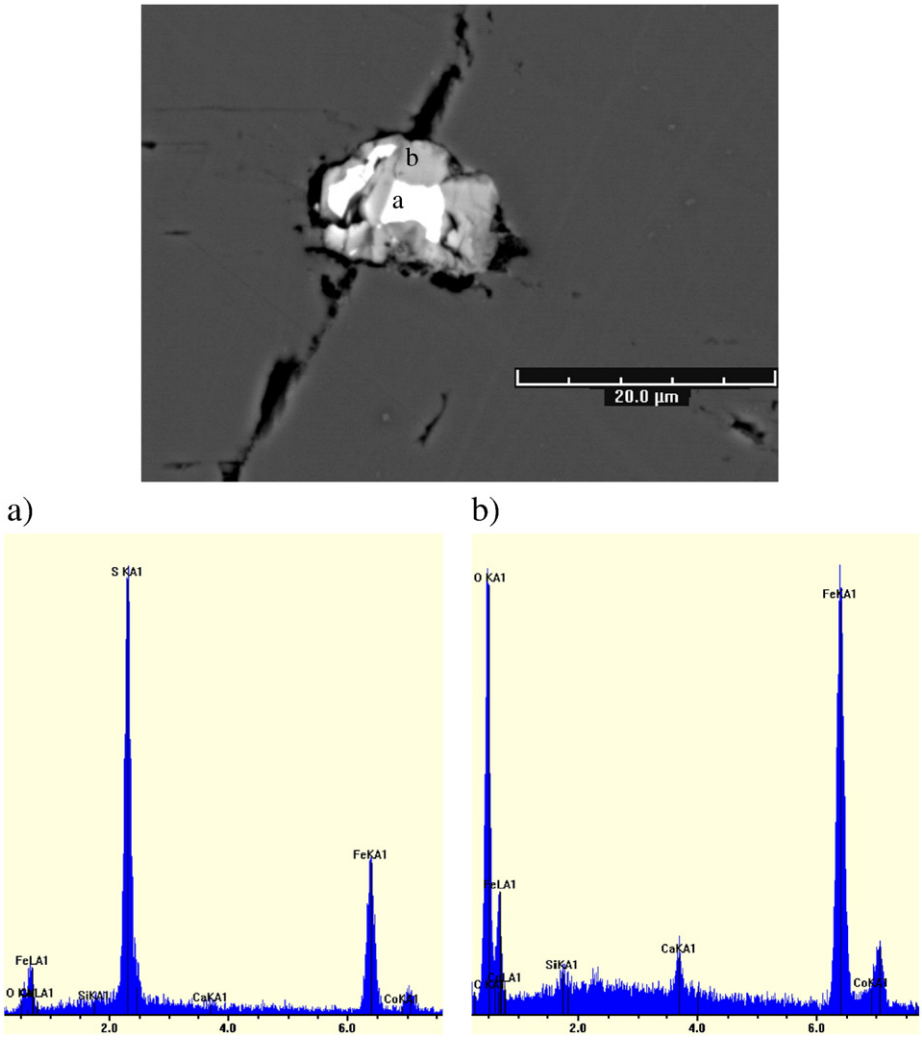

Fig. 6. Backscattered electron image (BSE) of an iron sulfide particle in the aggregate and EDS spectra of (a) bright area and b) darker area.

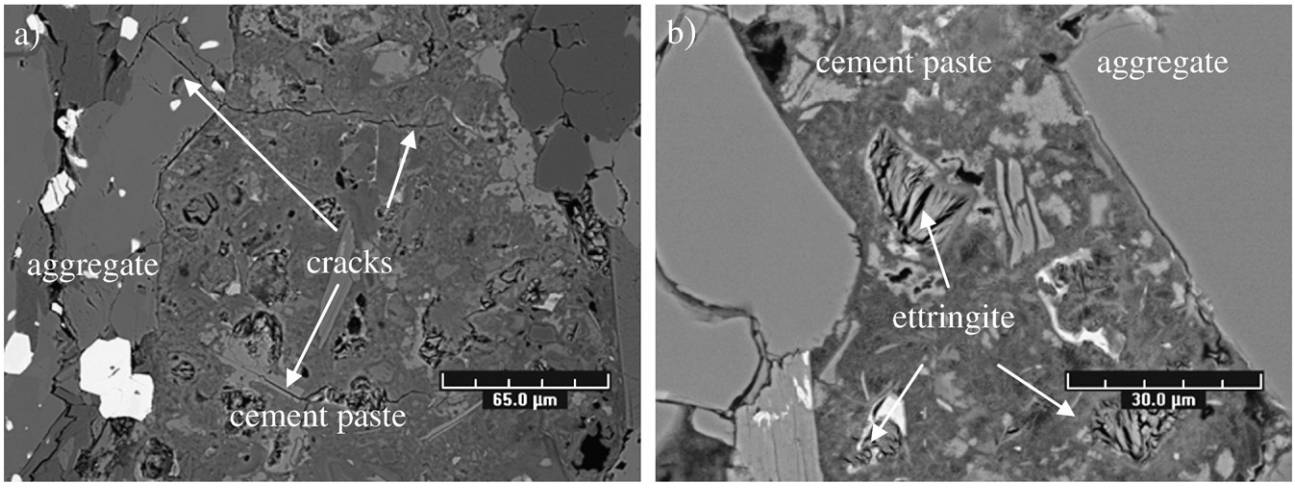

Fig. 7. Backscattered electron images (BSE) of concrete matrix with (a) cracks in aggregates and cement paste and (b) secondary ettringite deposits in the cement paste both from dam concrete after more than 40 years of natural weathering.

into the cement paste (Fig. 7). Thus, it appears that the degradation can be directly linked to the reaction of iron sulphides, which leads to an increase in volume within the aggregates that in turn crack and expand the concrete [8]. However, it should be noted that some minor cracks in the aggregates caused by the iron sulfides particles might have been present in the aggregates before the concrete was made originating from natural weathering effects. It should be noted that the investigated aggregates showed no or only a very little ASR reactivity.

The degree of reaction of the iron sulfides did seem to be related to the position of the particles within the aggregates. Particles close to the surface of the aggregates showed a higher degree of reaction than those near the center. It also looked like some cracking of the aggregates along grain boundaries contributed to higher degrees of reaction, possibly by facilitating the ingress of oxygen (Fig. 8). However, the extent of reaction did not appear to be related to the position in the structure, i.e., particles in aggregates near to the surface of the dam did not appear to be more reacted than those far from the surface (even 3 to 4 m) in to the dam.

The results further showed that the iron monosulfide had a much higher degree of reaction with about 60% by volume than the iron disulfide with only about 4% of reaction by volume as indicated in Fig. 4. It was concluded that under similar conditions, the iron monosulfide has a higher expansion potential in the concrete structure especially at the earlier stages of degradation.

Generally, the specific volume increase of the degrading iron sulfides can be calculated and theoretically increase up to 1.3, respectively, 1.7 times (Fig. 9). When it is assumed that the entire amount of iron sulfides degrades to half goethite (FeO(OH)) and half iron hydroxide ($Fe(OH)_3$), the maximum expansion of the aggregates can be calculated to be 0.07%. It should be noted that these critical expansion values are larger than the intrinsic strain limits of the aggregates, which are between 0.016% and 0.018% [15]. Beyond these critical values, the expansion starts to develop stress, which leads to cracks within the aggregates and finally cracks propagate into the cement paste. Thereby, already small iron sulfide particles can provide enough stress to crack the aggregate in the concrete matrix.

If the degree of reaction of the iron sulfides (Table 2), the resulting volume increase (Fig. 9), and the aggregate content in the concrete (about 75%) are taken into account, the resulting strain of the dam concrete can be assessed to be in the range of 0.04% to 0.05%. This about twice the actual expansion recorded. Consequently, iron sulfide

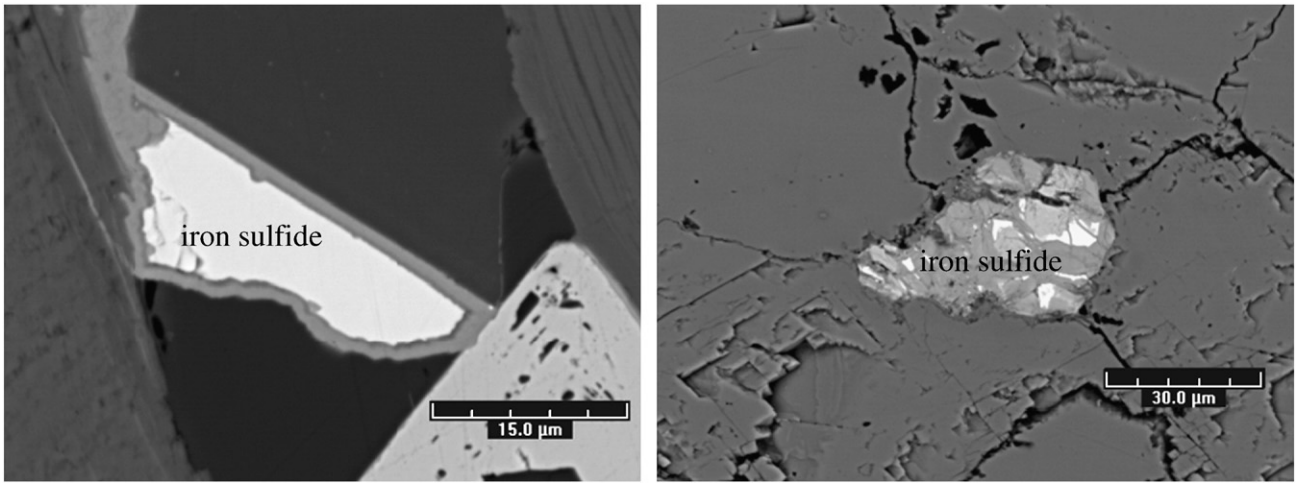

Fig. 8. Backscattered electron images (BSE) of partly reacted iron sulfide particles in aggregates depending on their accessibility within the concrete matrix after 40 years of natural weathering.

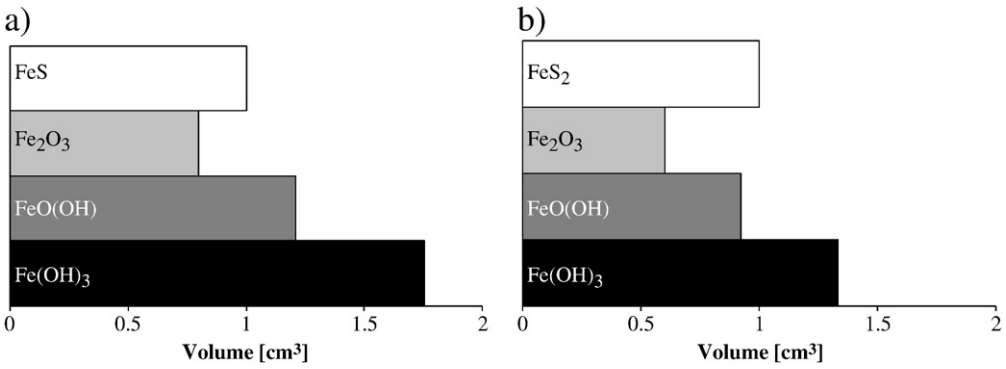

Fig. 9. Calculated theoretical volume change of 1 cm^3 of (a) pyrrhotide (FeS) and (b) pyrite (FeS_2) during the oxidation/degradation process involving oxygen and moisture.

degradation may be the main factor leading to the expansion of the dam and reactions such as secondary ettringite formation may contribute in a minor way (see following section).

However, it should be noted that the expansion of the concrete is not homogeneous. The expansion of small inclusions inside aggregates may actually magnify the volume increase of the inclusions.

3.3.2. Secondary ettringite

In the cement paste widespread deposits of ettringite were observed, mostly formed within the boundaries of the former clinker grains, the so-called inner product (Fig. 7b). Secondary ettringite due to the release of sulfate from the iron sulfides inclusions might mainly form close to residual aluminate sources [16]. These secondary ettringite deposits in the cement paste are typical for sulfate attack [17]. The amount of released SO_3 by iron sulfide degradation can be calculated approximately. At a reaction degree of 60% (Table 2), FeS in the concrete aggregate can release about 4.5 kg/m^3 of SO_3 into the paste. This correlates to an increase of SO_3 concentration in the cement paste (cement content of 280 kg/m^3) by 1.6%. The original sulfate content of the cement is not known but would probably have been around 2.5%. Therefore, the total sulfate level could be up to 4.1% after release of sulfate from the iron sulfides. If present from the start, this level of sulfate addition would still be below that needed to cause expansion.

The ettringite formed in the microstructure, either from normal hydration or from the additional sulfate released from the iron sulfides, can be clearly identified in porous regions of the microstructure, mainly inside the shells left by hydrating grains. There is no evidence of distress around such deposits, however, even in systems where expansion due to internal sulfate attack is known to occur [17], these large deposits of ettringite are not believed to be the origin of expansion. Instead expansion is believed to arise from the reaction of submicroscopic crystals of calcium alumina monosulfate (monosulfate), within the C–S–H to form ettringite. The signature of expansion related to such internal sulfate attack is the formation of gaps around the aggregates as the expanding paste expands away from the non-expanding aggregates [16]. In this case, there are no obvious gaps present. Nevertheless, we have to be careful about interpreting this as evidence that there is no expansion in the paste phase. First the expansions here are very low (a few hundredths of a percent), so the predicted gaps would hardly be visible and secondly, as already discussed, it is likely that the aggregates are expanding too in this case. Due to these factors, it is difficult to conclude about the contribution of ettringite formation from release of sulfates to the expansion of the concretes.

Table 2
Summary of results for the quantification of the iron sulfides comparing quarried and extracted aggregates with SEM microscopy and EDS analysis.

	Type of ore [% by volume]	
	FeS	FeS_2
Total amount	0.28	
Relative amounts	80	20
Totally reacted[a]	30 – 40	
Specifically reacted[a]	60	4

[a] Reacted after 40 years of natural weathering.

4. Conclusions

The examination of the concrete produced with aggregates containing iron sulfides clearly show that the formation of iron hydroxides can lead to expansion of particles within the aggregates, which leads to cracking of the aggregate. Approximate calculations indicate that this alone could account for the expansion observed on a macroscopic scale. This pattern of cracking in aggregates leading to overall expansion is similar to that observed in many cases of alkali silica reactions [14] and observed mechanisms are similar to the mechanisms that are known in the case of alkali silica reaction and can even act as a precursor for the iron sulfide degradation.

The investigations showed that the main iron sulfides present in the aggregates were pyrrhotite (FeS) and pyrite (FeS_2). It was found that pyrrhotite reacts much faster than pyrite in alkaline concrete environments. In combination with the larger amounts of FeS present in the concrete aggregates, its expansion potential for the dam concrete is much higher.

The reaction kinetics of the iron sulfides was generally very slow with only 30% to 40% or materials reacted after 40 years of natural weathering in the dam concrete and even smaller degree of reaction observed in the laboratory samples stored for 5 years at 40 and 60 °C. These findings indicate the difficulties to reproduce the specific iron sulfide degradation in the laboratory scale.

The formation of secondary ettringite, from released sulfate, was observed, but there were no clear signs of expansion associated with the extra sulfate. It is not clear to what extent this may contribute to the macroscopic reactions.

Acknowledgments

The authors would like to thank Axpo Group and Dr. Bastian Otto for financial support and guidance during the studies. Gwenn Le Saoût, Philip Vulliemin, and Phillip Simonin are thanked for their assistance in the experimental part of this study.

References

[1] M.D.A. Thomas, R.J. Kettle, J.A. Morton, Expansion of Cement-Stabilized Minestone due to the Oxidation of Pyrite, Geotechnical Engineering, Transportation Research Record 1219, 1989, pp. 113–120.

[2] K.J. Edwards, B.M. Goebel, T.M. Rodgers, M.M. Cardona, N.R. Pace, Geomicrobiology of pyrite (FeS_2) dissolution: case study at Iron Mountain, California, Geomicrobiol. J. 16 (1999) 155–179.
[3] I. Casanova, A. Aguada, L. Agullo, Aggregate expansivity due to sulfide oxidation—II. Physio-chemical modeling of sulfate attack, Cem. Concr. Res. 27 (1997) 1627–1632.
[4] H. Lee, R.D. Cody, A.M. Cody, P.G. Spry, The formation and role of ettringite in Iowa highway concrete deterioration, Cem. Concr. Res. 35 (2005) 332–343.
[5] M.A. Czerewko, J.C. Cripps, J.M. Reid, C.G. Duffell, Sulfur species in geological materials—sources and quantification, Cem. Concr. Res. 35 (2003) 657–671.
[6] J.S. Chinchon, Influence of weathering of iron sulfides contained in aggregates on concrete durability, Cem. Concr. Res. 25 (1995) 1264–1272.
[7] L. Divat, J.-P. Davy, Étude des risques d'oxidation de la pyrite dans le milieu basique du béton, Bull. Lab. ponts chaussées 4019 (1996) 97–107.
[8] M.D.A. Thomas, R.J. Kettle, J.A. Morton, The oxidation of pyrite in cement stabilized colliery shale, Q. J. Eng. Geol. 22 (1989) 2007–2218.
[9] G. Hu, K. Dam-Johansen, S. Wedel, J.P. Hansen, Decomposition and oxidation of pyrite, Prog. Energy Combust. Sci. 32 (2006) 295–314.
[10] M.A. Mckibben, H.L. Barnes, Oxidation of pyrite in low temperature acidic solutions: rate laws and surface textures, Geochem. Cosmochim. 50 (1986) 1509–1520.
[11] A.M. Marion, J. Daube, R. Smitz, The stability of pyrite in calcereous aggregate: investigations in old concrete structures, Proc. Third Annual International Conference on Cement Microscopy, Albuquerque, New Mexico, 2001, pp. 146–164.
[12] D. Borah, M. Barua, M.K. Baruah, Dependence of pyrite concentration on kinetics and thermodynamics of coal pyrolysis in non-isothermal systems, Fuel Process. Technol. 86 (2005) 977–993.
[13] C. Ayora, S. Chinchon, A. Aguada, Weathering of iron sulfides and concrete alteration: thermodynamic model and observation in dams from central pyrenees, spain, Cem. Concr. Res. 28 (1998) 591–603.
[14] M. BenHaha, Mechanical effects of alkali silica reaction in concrete studied by SEM-image analysis. PhD thesis. École Polytechnique Fédérale de Lausanne, Lausanne, 2006.
[15] M. Ben Haha, E. Gallucci, A. Guidoum, K.L. Scrivener, Relation of expansion to alkali silica reaction to the degree of reaction measured by SEM image analysis, Cem. Concr. Res. 37 (2007) 1206–1214.
[16] H.F.W. Taylor, C. Famy, K.L. Scrivener, Delayed ettringite formation, Cem. Concr. Res. 31 (2001) 683–693.
[17] T. Schmidt, B. Lothenbach, M. Romer, J. Neuenschwander, K. Scrivener, Physical and microstructural aspects of sulfate attack on ordinary and limestone blended Portland cements, Cem. Concr. Res. 39 (2009) 1111–1121.